Microstrip Antennas Integrated With Electromagnetic Band-Gap (EBG) Structures: A Low Mutual Coupling Design for Array Applications

Fan Yang, *Member, IEEE,* and Yahya Rahmat-Samii, *Fellow, IEEE*

***Abstract*—Utilization of electromagnetic band-gap (EBG) structures is becoming attractive in the electromagnetic and antenna community. In this paper, a mushroom-like EBG structure is analyzed using the finite-difference time-domain (FDTD) method. Its band-gap feature of surface-wave suppression is demonstrated by exhibiting the near field distributions of the electromagnetic waves. The mutual coupling of microstrip antennas is parametrically investigated, including both the E and H coupling directions, different substrate thickness, and various dielectric constants. It is observed that the E-plane coupled microstrip antenna array on a thick and high permittivity substrate has a strong mutual coupling due to the pronounced surface waves. Therefore, an EBG structure is inserted between array elements to reduce the mutual coupling. This idea has been verified by both the FDTD simulations and experimental results. As a result, a significant 8 dB mutual coupling reduction is noticed from the measurements.**

***Index Terms*—Electromagnetic band-gap (EBG), finite-difference time-domain (FDTD) method, microstrip antennas, mutual coupling, surface wave.**

I. Introduction

In RECENT years, there has been growing interest in utilizing electromagnetic band-gap (EBG) structures in the electromagnetic and antenna community. The EBG terminology has been suggested in [1] based on the photonic band-gap (PBG) phenomena in optics [2] that are realized by periodical structures. There are diverse forms of EBG structures [1], [3], and novel designs such as EBG structures integrated with active device [4] and multilayer EBG structures [5] have been proposed recently. This paper focuses on a mushroom-like EBG structure, as shown in Fig. 1. Compared to other EBG structures such as dielectric rods and holes, this structure has a winning feature of compactness [6], [7], which is important in communication antenna applications. Its band-gap features are revealed in two ways: the suppression of surface-wave propagation, and the in-phase reflection coefficient. The feature of surface-wave suppression helps to improve antenna's performance such as increasing the antenna gain and reducing back radiation [8]–[11]. Meanwhile, the in-phase reflection feature leads to low profile antenna designs [12]–[14].

This paper concentrates on the surface-wave suppression effect of the EBG structure and its application to reduce the mutual coupling of microstrip antennas, as shown in Fig. 1. To explore the surface-wave suppression effect, the propagating fields of an infinitesimal dipole source with and without the EBG structure are simulated and compared using the finite-difference time-domain (FDTD) method [15], and a frequency stopband for the field propagation is identified. Furthermore, the propagating near fields at frequencies inside and outside the band gap are graphically presented for a clear understanding of the physics of the EBG structure. It is worthwhile to point out that this band-gap study is closely associated with specific antenna applications such as microstrip antennas and arrays.

Applications of microstrip antennas on high dielectric constant substrates are of special interest due to their compact size and conformability with the monolithic microwave integrated circuit (MMIC). However, the utilization of a high dielectric constant substrate has some drawbacks. Among these are a narrower bandwidth and pronounced surface waves. The bandwidth can be recovered using a thick substrate, yet this excites severe surface waves. The generation of surface waves decreases the antenna efficiency and degrades the antenna pattern. Furthermore, it increases the mutual coupling of the antenna array which causes the blind angle of a scanning array. Several methods have been proposed to reduce the effects of surface waves. One approach suggested is the synthesized substrate that lowers the effective dielectric constant of the substrate either under or around the patch [16]–[18]. Another approach is to use a reduced surface wave patch antenna [19]. The EBG structures are also used to improve the antenna performance. However, most researchers only study the EBG effects on a single microstrip antenna element, and to the best of our knowledge there are no comprehensive results reported for antenna arrays.

The FDTD method is developed to analyze the mutual coupling of probe-fed microstrip patch antenna arrays. The simulated results agree well with the experimental results in [20]. Then, the mutual coupling of microstrip antennas is parametrically investigated, including both the E- and H-coupling directions, different substrate thickness, and various dielectric constants. In both coupling directions, increasing the substrate thickness will increase the mutual coupling. However, the effect of the dielectric constant on mutual coupling is different at various coupling directions. It is found that for the E-plane coupled cases the mutual coupling is stronger on a high permittivity substrate than that on a low permittivity substrate. In contrast, for the H-plane coupled cases the mutual coupling

Manuscript received January 29, 2002; revised November 25, 2002.

The authors are with the Department of Electrical Engineering, University of California at Los Angeles, Los Angeles, CA 90095-1594 USA (e-mail: ygfn@ee.ucla.edu; rahmat@ee.ucla.edu).

Digital Object Identifier 10.1109/TAP.2003.817983

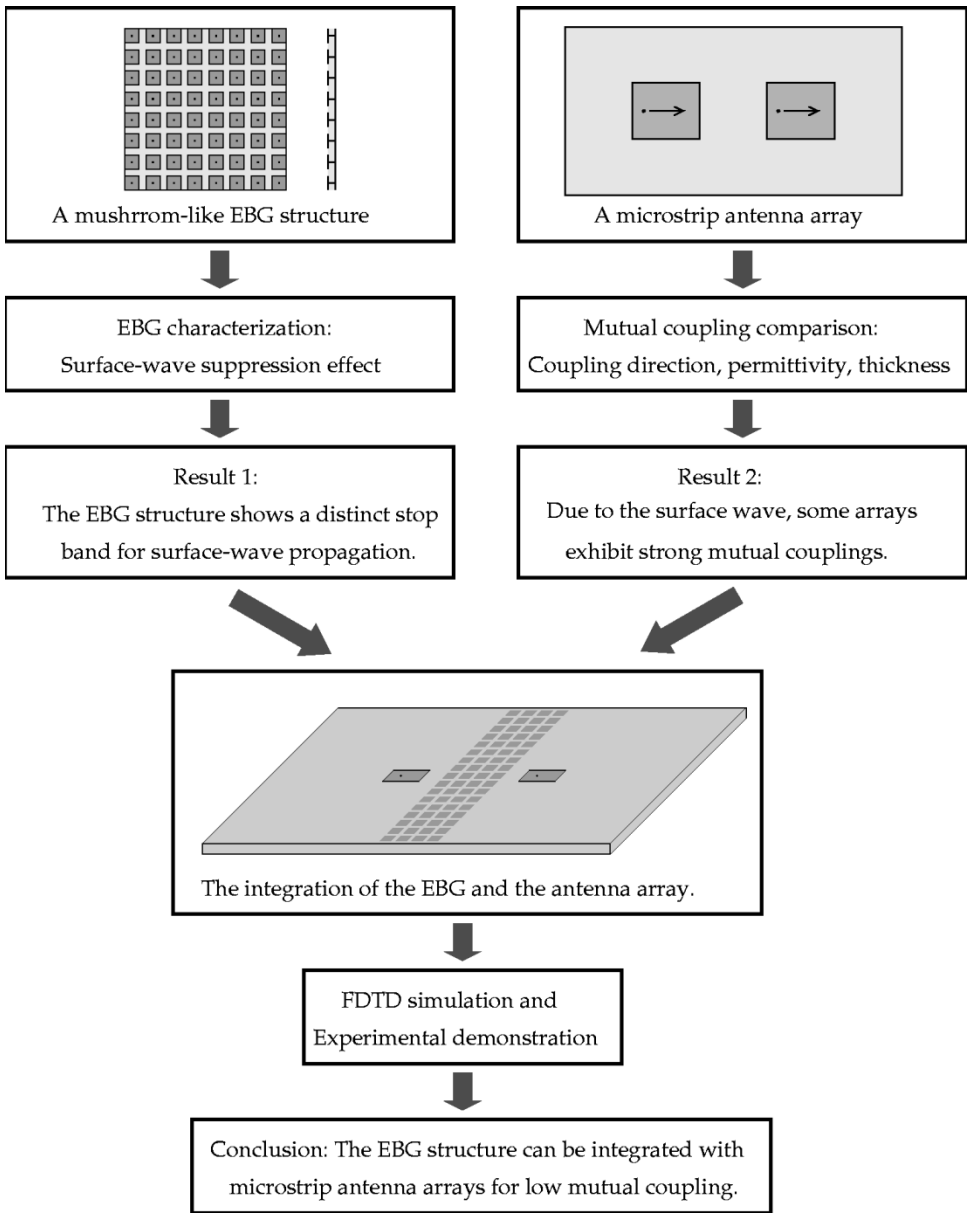

Fig. 1. Integration of the EBG structure with microstrip antenna array for reduced mutual coupling.

is weaker on a high permittivity substrate than that on a low permittivity substrate. This difference is due to surface waves propagating along the E-plane direction, which can be easily viewed from the provided near field plots.

To reduce the strong mutual coupling of the E-plane coupled microstrip antennas on a thick and high permittivity substrate, the mushroom-like EBG structure is inserted between antenna elements. When the EBG parameters are properly designed, the pronounced surface waves are suppressed, resulting in a low mutual coupling. This method is compared with previous methods such as cavity back patch antennas. The EBG structure exhibits a better capability in lowering the mutual coupling than those approaches. Finally, several antennas with and without the EBG structure are fabricated on Rogers RT/Duroid 6010 substrates ($\epsilon_r = 10.2$). The measured results demonstrate the utility of the EBG structure, and this approach is potentially useful for a variety of array applications.

II. Band Gap Characterization of the EBG Structure

The mushroom-like EBG structure was first proposed in [3]. It consists of four parts: a ground plane, a dielectric substrate, metallic patches, and connecting vias. This EBG structure exhibits a distinct stopband for surface-wave propagation.

The operation mechanism of this EBG structure can be explained by an LC filter array: the inductor L results from the current flowing through the vias, and the capacitor C due to the gap effect between the adjacent patches. For an EBG structure with patch width W, gap width g, substrate thickness h and dielectric constant ϵ_r, the values of the inductor L and the capacitor C are determined by the following formula [21]:

$$L = \mu_0 h \tag{1}$$

$$C = \frac{W\epsilon_0(1+\epsilon_r)}{\pi}\cosh^{-1}\left(\frac{2W+g}{g}\right) \tag{2}$$

where μ_0 is the permeability of free space and ϵ_0 is the permittivity of free space.

Reference [21] also predicts the frequency band gap as

$$\omega = \frac{1}{\sqrt{LC}} \tag{3}$$

$$BW = \frac{\Delta\omega}{\omega} = \frac{1}{\eta}\sqrt{\frac{L}{C}} \tag{4}$$

where η is the free space impedance which is 120π.

These formulations are very simple; however, their results are not very accurate. For example, this model does not consider the via's radius information. An accurate but complex model using the theory of transmission lines and periodic circuits can be found in [22]. Some other methods such as reflection phase characterization have also been utilized to identify the band-gap features [23].

In this paper, to accurately identify the band-gap region and understand its properties comprehensively, the FDTD method is used to analyze the band-gap features. The computational code developed in UCLA is based on a Cartesian grid cell with the perfectly matched layer (PML) boundary condition. A uniform 0.02 $\lambda_{6\text{ GHz}}$ ($\lambda_{6\text{ GHz}}$ is the free space wavelength at 6 GHz) discretization is used. An infinitesimal dipole source with a Gaussian pulse waveform is utilized to activate the structure in order to obtain a wide range of frequency responses.

Fig. 2(a) shows an FDTD simulation model: the infinitesimal dipole source surrounded by the mushroom-like EBG structure. The dipole is chosen to be vertically polarized because the E field in microstrip antenna applications is vertical to the ground plane. As an example, two rows of EBG patches are plotted in Fig. 2(a). In FDTD simulations four rows, six rows, and eight rows of EBG patches are all simulated and compared.

The EBG structure analyzed in this section has the following parameters:

$$W = 0.12\lambda_{6\text{ GHz}}, \quad g = 0.02\lambda_{6\text{ GHz}},$$
$$h = 0.04\lambda_{6\text{ GHz}}, \quad \epsilon_r = 2.20. \tag{5}$$

The vias' radius is 0.005 $\lambda_{6\text{ GHz}}$. The ground plane size is kept to be $2.84\lambda_{6\text{ GHz}} \times 2.84\lambda_{6\text{ GHz}}$. A reference plane is positioned at $0.12\lambda_{6\text{ GHz}}$ distance away from the edge, where it is located outside the EBG structure, and the height of the reference plane is $0.04\lambda_{6\text{ GHz}}$. For the sake of comparison, a conventional case is also analyzed. This conventional (CONV.) case consists of a perfect electric conductor (PEC) ground plane and a dielectric substrate with the same thickness and permittivity as the EBG case.

The basic idea is to calculate and compare the E field at the reference plane. Since the EBG structure can suppress the surface waves in a certain band gap, the E field outside the EBG structure should be weaker than that of the conventional case. To quantify the surface-wave suppression effect, an average $|\overline{E}|^2$ is calculated according to the following equation:

$$|\overline{E}|^2 = \frac{1}{S}\iint_S |E|^2\, ds \tag{6}$$

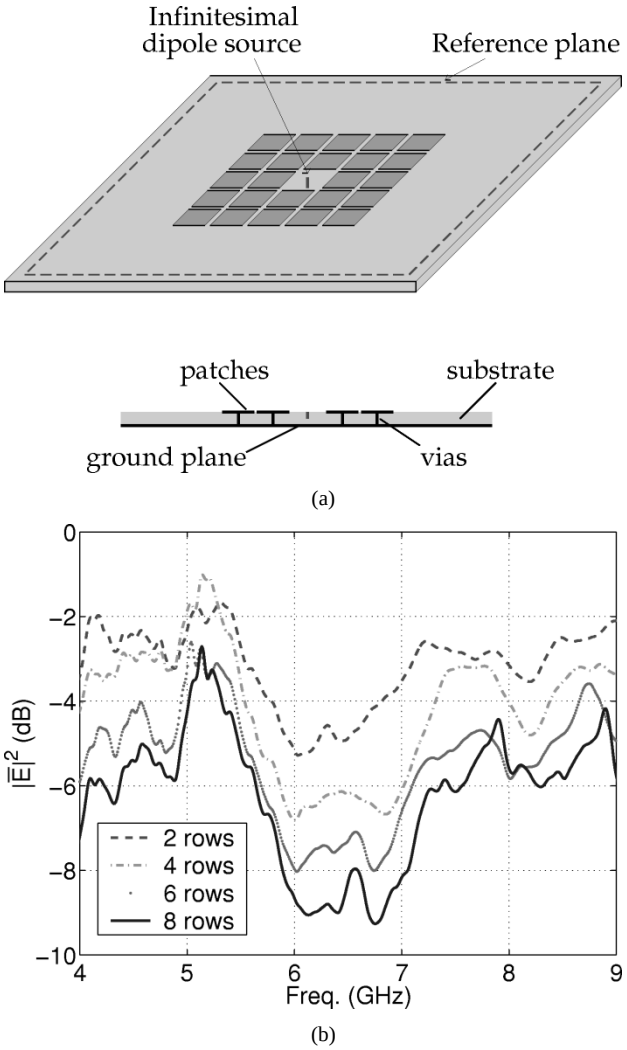

Fig. 2. EBG structure is analyzed using the FDTD method: (a) simulation model and (b) $|\overline{E}|^2$ at the reference plane. The $|\overline{E}|^2$ of various EBG cases are normalized to the $|\overline{E}|^2$ of the conventional case.

where S is the vertical reference plane whose boundary is plotted by the dashed line in Fig. 2(a).

Fig. 2(b) plots the $|\overline{E}|^2$ of various EBG cases and they are normalized to the $|\overline{E}|^2$ of the conventional case. A parametric study analyzing the number of EBG rows is carried out varying the number of rows from two to eight. It is observed that when less rows of EBG patches are used, the band-gap effect is not significant. When the number of rows is increased, a clear band gap can be noticed. Inside this band gap, the average E field in the EBG case is much lower than that in the conventional case. To determine the band-gap region, a criteria is used that the average E field magnitude with the EBG is less than half of that without the EBG (the CONV. case). This is equivalent to the -6 dB ($10\log_{10}|\overline{E}|^2$) level in Fig. 2(b), thus a band gap from 5.8–7.0 GHz can be identified with a minimum of four rows of EBG patches.

The LC model [(1)–(4)] is also used to analyze this mushroom-like EBG structure, and a band gap of 6.37–8.78 GHz is obtained. It has some overlap with the band gap calculated by the FDTD method, which means this model can be used to get an initial engineering estimation. However, the LC model result

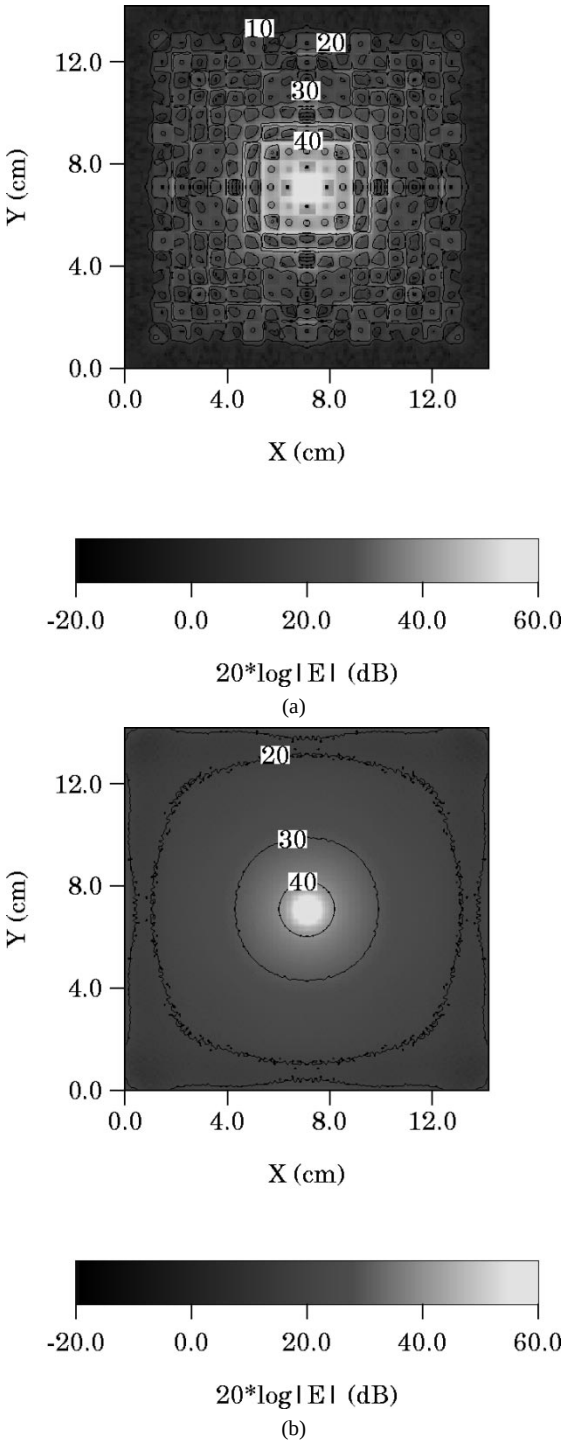

Fig. 3. Near fields at 6 GHz, which is inside the band gap. (a) The EBG case and (b) the CONV. case. The outside field of the EBG case is about 10 dB lower than that of the CONV. case because of the surface-wave suppression.

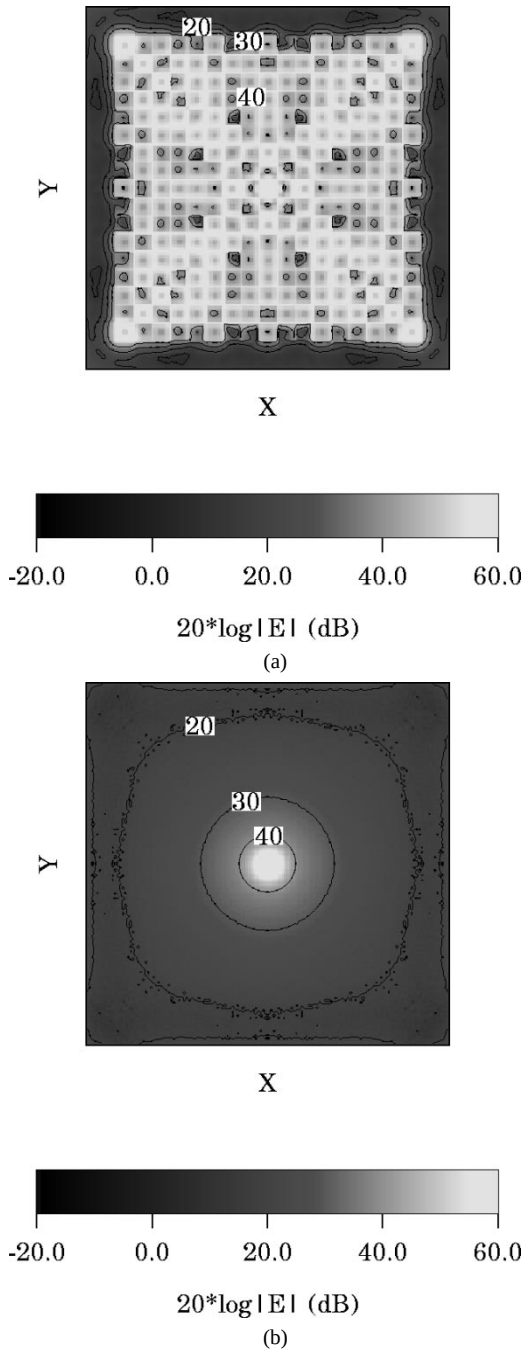

Fig. 4. Near fields at 5 GHz, which is outside the band gap. (a) The EBG case and (b) the CONV. case. The outside field of the EBG case has a similar level as that of the CONV. case.

is relatively higher than the FDTD results because it uses a simplified lumped element model. This is also the reason to develop the FDTD model here.

To visualize the band-gap feature of surface-wave suppression, the near field distributions of the eight row EBG case and the conventional case are calculated and graphically presented. Fig. 3 plots the near field of both cases at 6 GHz, which is inside the band gap. The field level is normalized to 1 W delivered power and is shown in dB scale. The field level outside the EBG structure is around 10 dB. In contrast, the field level of the CONV. case is around 20 dB. The difference of field levels is due to the existence of the EBG structure, which suppresses the propagation of surface waves so that the field level in the EBG case is much lower than in the conventional case. However, the EBG structure cannot successfully suppress surface waves outside its frequency band gap. For example, Fig. 4 plots the near field of both cases at 5 GHz, which is outside the band gap. The field distribution of the CONV. case is similar to its distribution at 6 GHz. However, the field value outside the EBG structure is increased to around 20 dB, which is similar to that of the CONV.

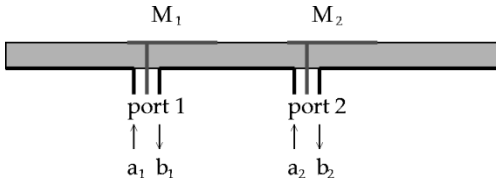

Fig. 5. FDTD model to calculate the mutual coupling of probe fed microstrip antennas.

case. This means that although there are some interactions between the dipole source and the EBG structure, the field can still propagate through the EBG structure. These results correlate well with the results in Fig. 2(b). From this comparison it can be concluded that as expected, the surface-wave suppression effect exists only inside the band gap of the EBG structure.

III. Mutual Coupling Comparison of Various Microstrip Antenna Arrays

A. FDTD Method for Mutual Coupling Simulation

The FDTD method is used to analyze the mutual coupling of microstrip antennas. The mutual coupling of antennas fed by microstrip lines has been solved using the FDTD method in [24], and the probe fed antenna case is discussed herein.

Fig. 5 plots an FDTD model to calculate the mutual coupling of two probe fed patch antennas. The reflection coefficients are defined as

$$\begin{bmatrix} b_1 \\ b_2 \end{bmatrix} = \begin{bmatrix} S_{11} & S_{12} \\ S_{21} & S_{22} \end{bmatrix} \begin{bmatrix} a_1 \\ a_2 \end{bmatrix} \tag{7}$$

where a_1, a_2, b_1, and b_2 are the normalized voltage waves. The incident wave and reflected waves are mixed together during the FDTD simulation, and the voltages and currents are recorded at the ports [15]. The relation between the waves and the recorded data is

$$V_1 = \sqrt{Z_{c1}}(a_1 + b_1) \tag{8}$$

$$I_1 = \frac{1}{\sqrt{Z_{c1}}}(a_1 - b_1) \tag{9}$$

$$V_2 = \sqrt{Z_{c2}}(a_2 + b_2) \tag{10}$$

$$I_2 = \frac{1}{\sqrt{Z_{c2}}}(a_2 - b_2) \tag{11}$$

where Z_{c1} and Z_{c2} are characteristic impedances of the feeding probes.

A Gaussian pulse type of voltage source is used to excite the structure. For simplicity, only port one is activated during the simulation and port two is matched to 50 Ω. Therefore, the incident wave at port two is zero, $a_2 = 0$. Thus, (7) becomes

$$b_1 = S_{11}a_1 \tag{12}$$

$$b_2 = S_{21}a_1. \tag{13}$$

Substituting (12) and (13) into (8)–(11) and dividing (8) and (10) by (9), one arrives at

$$\frac{V_1}{I_1} = Z_{c1}\frac{1 + S_{11}}{1 - S_{11}} \tag{14}$$

$$\frac{V_2}{I_1} = \sqrt{Z_{c2}Z_{c1}}\frac{S_{21}}{1 - S_{11}}. \tag{15}$$

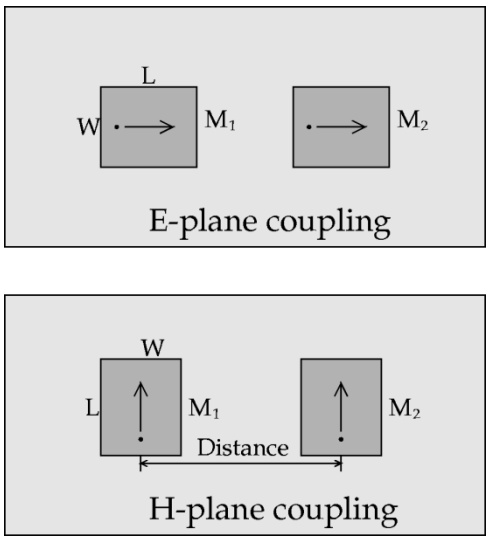

Fig. 6. E- and H-plane coupled probe fed microstrip antennas.

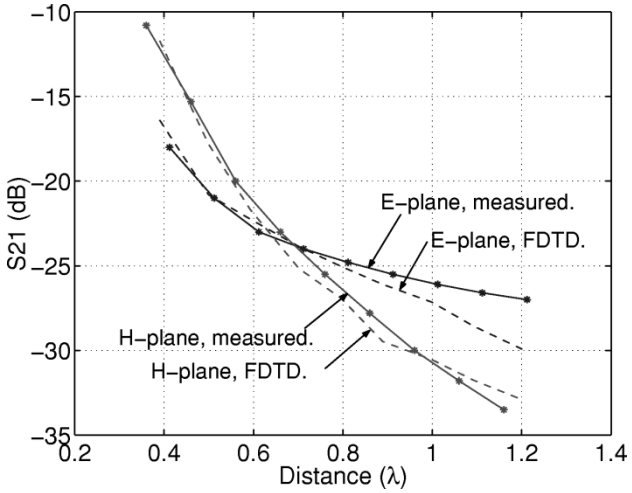

Fig. 7. Measured [20] and FDTD simulated mutual coupling results at 1.56 GHz for 5 cm (radiating edge) × 6 cm patches on a 0.305 cm thick substrate with a dielectric constant of 2.5.

Once the voltages and currents are obtained, the return loss (S_{11}) and mutual coupling (S_{21}) can be derived from (14) and (15).

The validity of these formulations has been demonstrated by the E-plane and H-plane coupled microstrip antennas illustrated in Fig. 6. A comparison of FDTD simulation results and experimental results [20] is shown in Fig. 7. The antenna has a patch size of 5 cm (radiation edge) × 6 cm, and is mounted on a 0.305 cm substrate with a dielectric constant of 2.5. The mutual coupling is calculated and measured at 1.56 GHz, and good agreements are observed. This method can also be used to analyze the mutual coupling of microstrip antennas with arbitrary orientation [25].

B. Mutual Coupling Comparison

The developed FDTD method is next used to analyze the mutual coupling features of microstrip antennas at different thicknesses and permittivities [26], [27]. Both the E-plane and H-plane couplings are investigated, and four patch antennas are compared as follows:

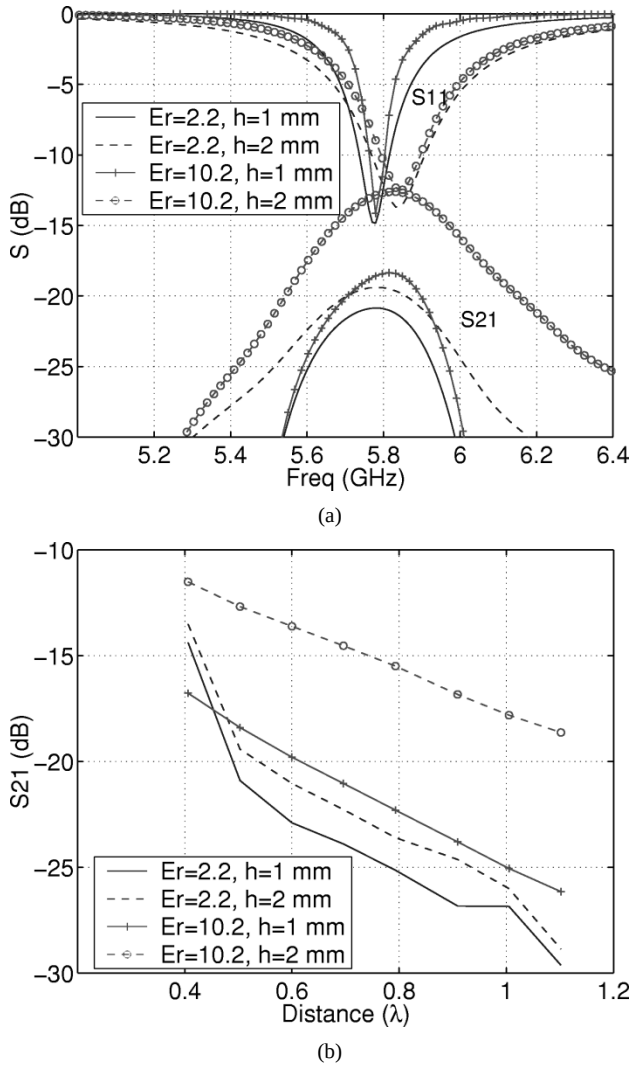

Fig. 8. Comparisons of the E-plane coupled microstrip antennas on different dielectric constants and different thickness substrates: (a) S_{11} and S_{21} versus frequency (distance = 0.5 $\lambda_{5.8\ \mathrm{GHz}}$), (b) S_{21} versus patch distance (f = 5.8 GHz).

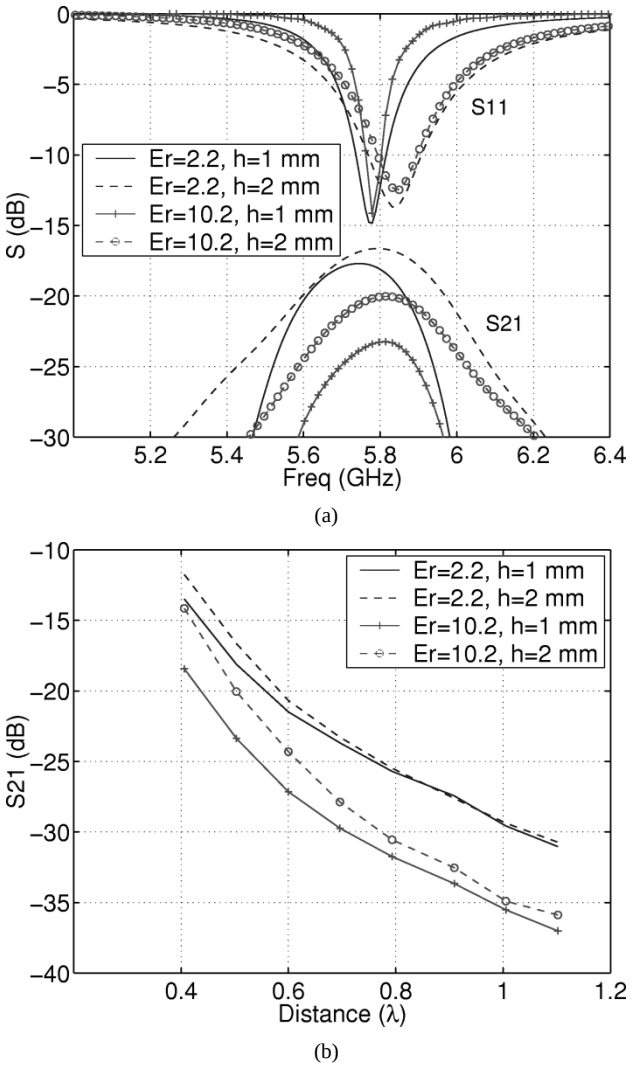

Fig. 9. Comparisons of the H-plane coupled microstrip antennas on different dielectric constants and different thickness substrates: (a) S_{11} and S_{21} versus frequency (distance = 0.5 $\lambda_{5.8\ \mathrm{GHz}}$), (b) S_{21} versus patch distance (f = 5.8 GHz).

1) patch antennas on a thin and low dielectric constant substrate: $\epsilon_r = 2.20$, $\mathrm{h} = 1$ mm, and the patch size is 16 mm $\times$ 9 mm;

2) patch antennas on a thick and low dielectric constant substrate: $\epsilon_r = 2.20$, $\mathrm{h} = 2$ mm, and the patch size is 15.5 mm $\times$ 12 mm;

3) patch antennas on a thin and high dielectric constant substrate: $\epsilon_r = 10.20$, $\mathrm{h} = 1$ mm, and the patch size is 7.5 mm $\times$ 5 mm;

4) patch antennas on a thick and high dielectric constant substrate: $\epsilon_r = 10.20$, $\mathrm{h} = 2$ mm, and the patch size is 7 mm $\times$ 4 mm.

The results of the E-plane coupled microstrip antennas are depicted in Fig. 8. Fig. 8(a) plots the return loss results of the four antenna cases. All the antennas are designed to resonate around 5.8 GHz. This frequency range is chosen for the ease of measurements to be presented in the next section. The impedance bandwidths (according to $S_{11} < -10$ dB criterion) are 1.38% for the first case, 2.40% for the second case, 0.61% for the third case, and 1.71% for the last case. It can be observed that the bandwidth increases with increasing thickness and decreases while the permittivity increases. It's worthwhile to point out that the bandwidth of case 4 is even larger than that of case 1, which means the bandwidth of microstrip antennas on a high permittivity substrate can be recovered by increasing the substrate thickness. Similar observations were also made in [18], which emphasized on a single element's performance, especially on the improvement of radiation patterns.

Fig. 8(a) also presents the mutual coupling of the E-plane coupled microstrip antennas with a 0.50 $\lambda_{5.8\ \mathrm{GHz}}$ antenna distance. $\lambda_{5.8\ \mathrm{GHz}}$ is the free space wavelength at the resonant frequency 5.8 GHz. The first case has the lowest mutual coupling level, while the last case shows the strongest. This is because the microstrip antenna on a high permittivity and thick substrate activate the most severe surface waves. Fig. 8(b) plots the mutual coupling varying with the patch distance at the resonant frequency. The mutual coupling of all cases decreases as the antenna distance increases. It is observed that both increasing the substrate thickness and permittivity will increase the mutual coupling level.

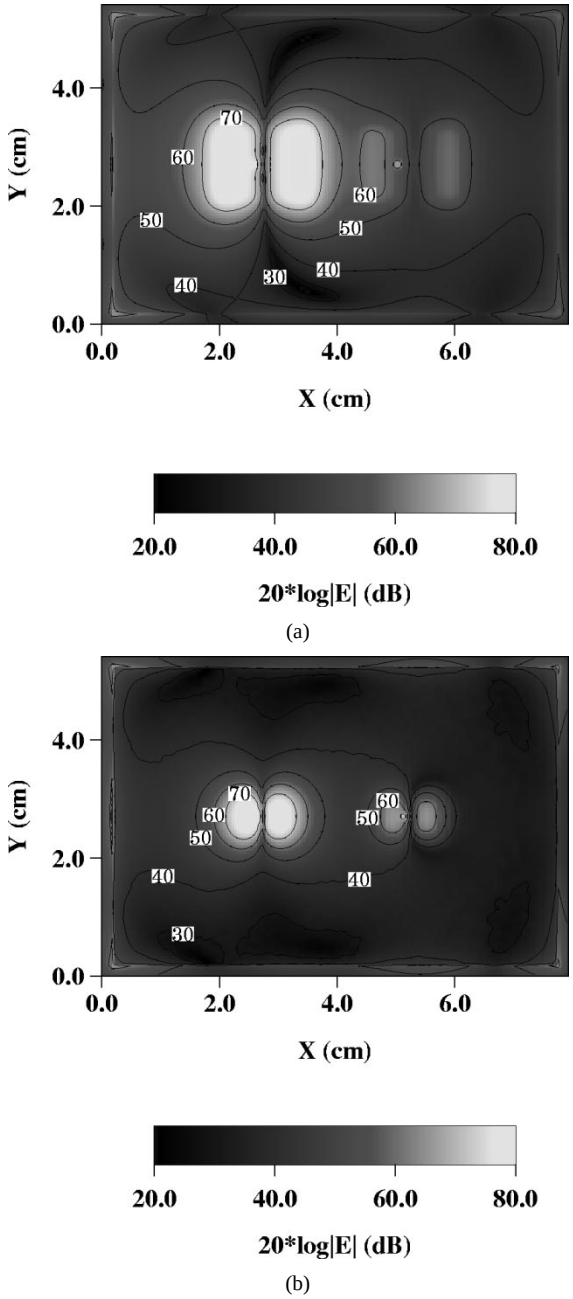

Fig. 10. Near fields of the E-plane coupled microstrip antennas on a 2 mm thick substrate: (a) $\epsilon_r = 2.20$ and (b) $\epsilon_r = 10.20$. The left antennas are activated and the mutual coupling is measured at the feeding port of the right antennas.

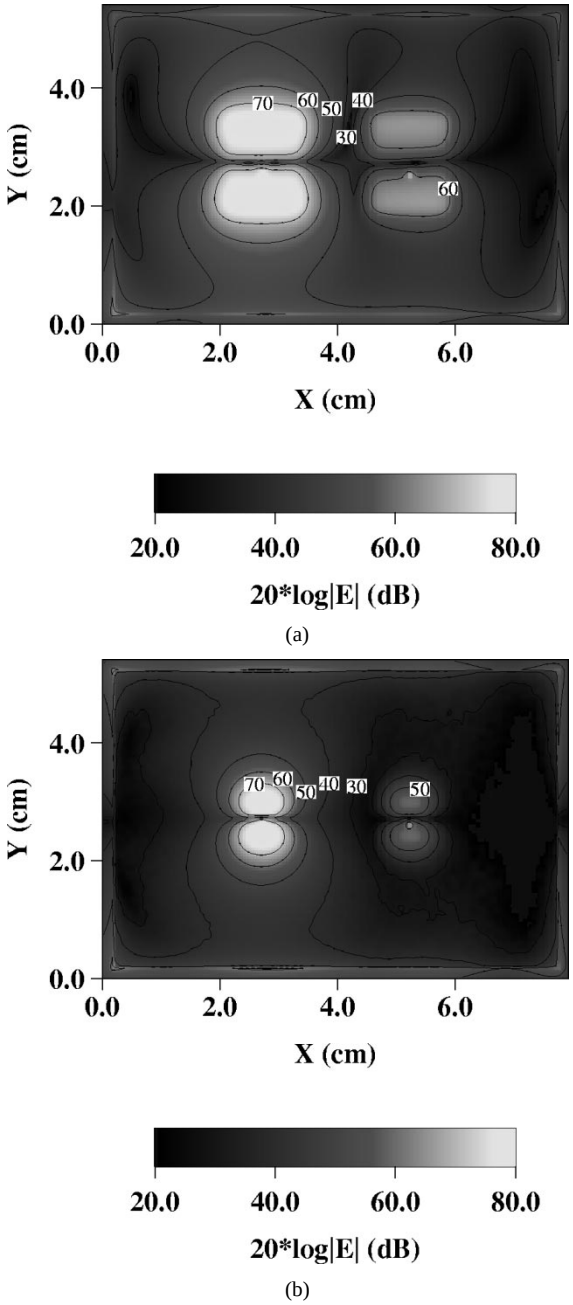

Fig. 11. Near fields of the H-plane coupled microstrip antennas on a 2 mm thick substrate: (a) $\epsilon_r = 2.20$ and (b) $\epsilon_r = 10.20$. The left antennas are activated and the mutual coupling is measured at the feeding port of the right antennas.

In Fig. 9, the H-plane coupled microstrip antennas results are depicted. Fig. 9(a) plots the return loss and mutual coupling versus frequency with a 0.50 $\lambda_{5.8\ \mathrm{GHz}}$ antenna distance, and Fig. 9(b) plots the mutual coupling varying with antenna distance at the resonant frequency 5.8 GHz. In contrast to the E-plane coupled results, the strongest mutual coupling occurs at the second case, which has a low dielectric constant and a thick substrate thickness, and the weakest mutual coupling happens at the third case, which has a high dielectric constant and a thin substrate thickness. It is observed that increasing the substrate thickness still increases the mutual coupling, while increasing the permittivity decreases it.

To identify the difference between the E-plane and H-plane coupled microstrip antenna arrays, the near fields of different coupling situations are calculated and graphically presented. Fig. 10 plots the near fields of the E-plane coupled microstrip antennas on a 2 mm thick substrate with (a) $\epsilon_r = 2.20$ and (b) $\epsilon_r = 10.20$. The left antennas (M1 in Fig. 6) are activated and the mutual coupling is measured at the feeding port of the right antennas (M2 in Fig. 6). The field is normalized to 1 W delivered power, and plotted in dB scale. The surface waves propagate along the X direction and a strong mutual coupling can be observed for the antennas on the high permittivity substrate. Fig. 11 shows the near fields of the H-plane coupled microstrip antennas. As

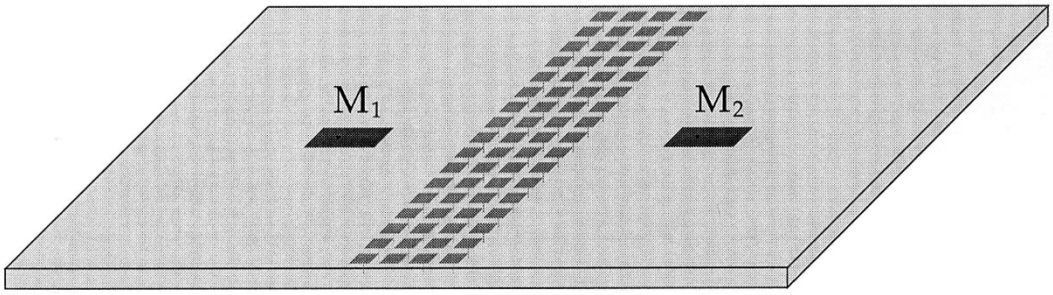

Fig. 12. Microstrip antennas separated by the mushroom-like EBG structure for a low mutual coupling. Four columns EBG patches are used.

shown in Fig. 11(a), the antennas on a low permittivity substrate have a larger patch size and their fringing fields couple to each other, resulting in a strong mutual coupling. However, for the antennas on a high permittivity substrate, there is less coupling between their fringing fields due to its small patch size shown in Fig. 11(b). The surface waves which contribute to the strong mutual coupling of the E-plane coupled case have less effect now because they do not propagate along the X direction. It can be concluded from the above discussion that the mutual coupling behaviors of microstrip antennas are determined by both the directional surface waves and antenna size.

IV. Mutual Coupling Reduction Using the EBG Structure

A. FDTD Simulation Results

From the above comparison, it is found that the E-plane coupled microstrip antennas on a thick and high permittivity substrate exhibit very strong mutual coupling due to the pronounced surface waves. Since the EBG structure has already demonstrated its ability to suppress surface waves, four columns of EBG patches are inserted between the antennas to reduce the mutual coupling, as shown in Fig. 12.

Fig. 13 shows FDTD simulated results of the E-plane coupled microstrip antennas on a dielectric substrate with $h = 2$ mm and $\epsilon_r = 10.2$. The antenna's size is 7mm $\times$ 4 mm, and the distance between the antennas is 38.8 mm ($0.75\lambda_{5.8\ \mathrm{GHz}}$). The mushroom-like EBG structure is inserted between the antennas to reduce the mutual coupling. Three different EBG cases are analyzed and their mushroom-like patch sizes are 2, 3, and 4 mm, respectively. The gap between mushroom-like patches is constant at 0.5 mm for all three cases.

Fig. 13(a) shows the return loss of three EBG cases, as well as the antennas without the EBG structure. It is observed that all the antennas resonate around 5.8 GHz. Although the existence of the EBG structure has some effects on the input matches of the antennas, all the antennas still have better than -10 dB matches.

The mutual coupling results are shown in Fig. 13(b). Without the EBG structure, the antennas show a strong mutual coupling of -16.15 dB. If the EBG structures are employed, the mutual coupling level changes. When the 2 mm EBG case is used, its band gap is higher than the resonant frequency 5.8 GHz. Therefore, the mutual coupling is not reduced and a strong coupling of -15.85 dB is still noticed. For the 3 mm EBG case, the resonant frequency 5.8 GHz falls inside the EBG band gap so that the surface waves

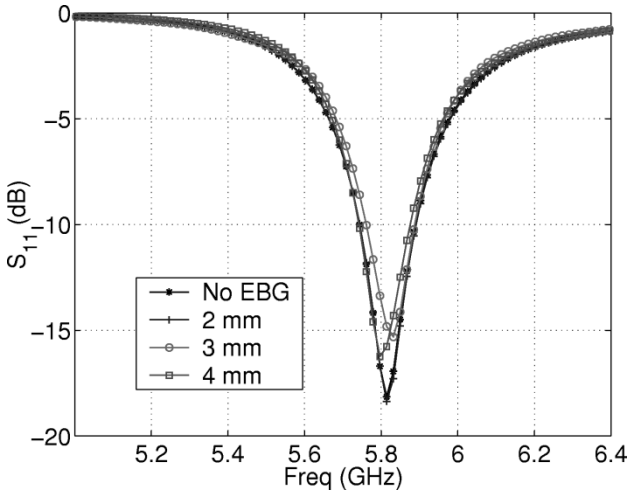

(a)

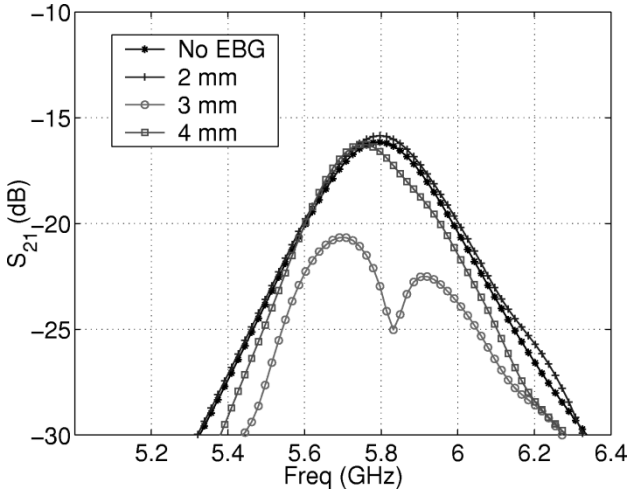

(b)

Fig. 13. FDTD simulated results of the E-plane coupled microstrip antennas separated by EBG structures with different mushroom-like patch sizes (2, 3, and 4 mm): (a) return loss and (b) mutual coupling.

are suppressed. As a result, the mutual coupling is greatly reduced: only -25.03 dB at the resonant frequency. It is worthwhile to point out that the bandwidth of the EBG structure is much wider than the antenna bandwidth so that it can cover the operational band of the antenna. When the size of the mushroom-like patch is increased to 4 mm, its band gap decreases, and is now lower than the resonant frequency. Therefore, the mutual coupling is not improved and is still as strong as -16.27 dB.

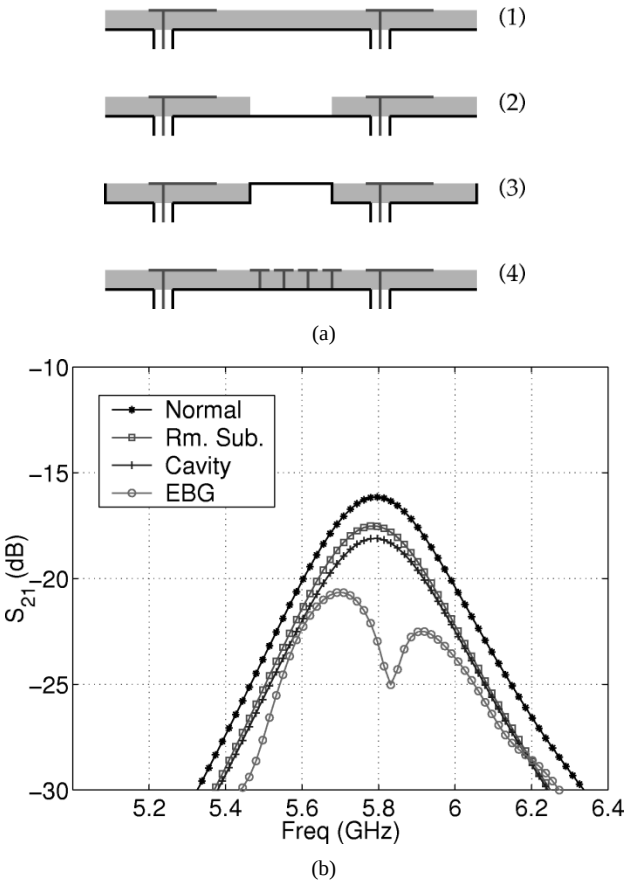

Fig. 14. Comparison of E-plane mutual coupling using different microstrip antenna structures. (a) Four different patch antenna structures: (1) normal microstrip antennas, (2) substrate between antennas is removed, (3) cavity back microstrip antennas, and (4) microstrip antennas with the EBG structure in between. (b) Mutual coupling results of four antenna structures. Patch antennas resonate at 5.8 GHz.

B. Comparison of the EBG Structure With Other Approaches

It is instructive to compare the EBG structure with other structures also used to reduce the mutual coupling. Fig. 14(a) plots four E-plane coupled antenna structures to be compared:

1) normal microstrip antennas,
2) the substrate between antennas are removed,
3) cavity back microstrip antennas, and
4) microstrip antennas with the EBG structure in between.

During the comparison, the antenna size, substrate properties, and antenna distance in all the structures are kept the same as in the EBG case. In structure 2), a 13.5 mm width substrate is removed between the patch antennas. This width is chosen to be the same as the total width of four rows of the EBG patches. When the cavity structure is used, the distance between the adjacent PEC wall is also selected to be 13.5 mm.

Fig. 14(b) displays the mutual coupling results of four different structures. The normal microstrip antennas show the highest mutual coupling. The substrate removal case and the cavity back case have some effects on reducing the mutual coupling. A 1.5 dB mutual coupling reduction is noticed for the former case and a 2 dB reduction is observed for the latter case. The lowest mutual coupling is obtained in the EBG case as an 8.8 dB reduction is achieved. This comparison demonstrates the unique capability of the EBG structure to reduce the mutual coupling.

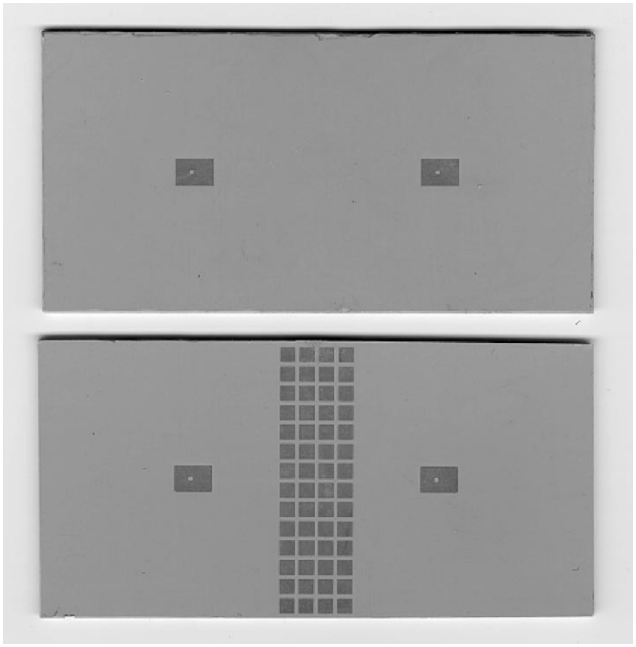

Fig. 15. Photo of microstrip antennas with and without the EBG structure. The substrate thickness is 1.92 mm and its dielectric constant is 10.2. The antenna size is 6.8 mm $\times$ 5 mm with a distance of 38.8 mm. The EBG mushroom-like patch size is 3 mm and the gap width is 0.5 mm.

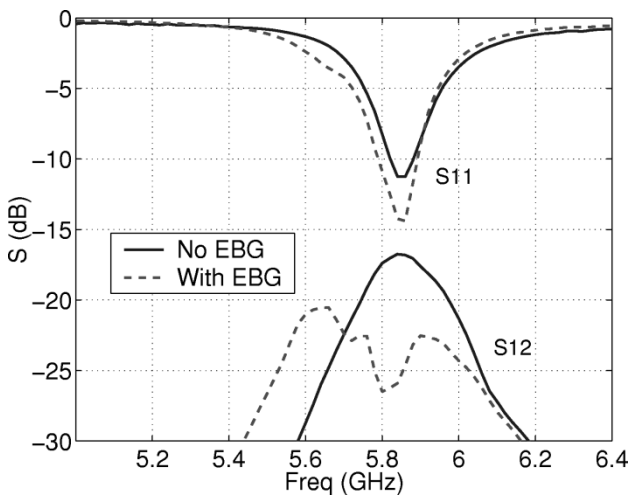

Fig. 16. Measured results of microstrip antennas with and without the EBG structure. An 8 dB mutual coupling reduction is observed at the resonant frequency.

C. Experimental Demonstration

To verify the conclusions drawn from the FDTD simulation, two pairs of microstrip antennas are fabricated on Roger RT/Duroid 6010 substrates. The permittivity of the substrate is 10.2, and the substrate thickness is 1.92 mm (75 mil). Fig. 15 shows a photograph of the fabricated antennas with and without the EBG structure. The antenna's size is 6.8 mm $\times$ 5 mm, and the distance between the antennas' edges is 38.8 mm (0.75 $\lambda_{5.8\mathrm{GHz}}$). The antennas are fabricated on a ground plane of 100 mm $\times$ 50 mm. For the EBG structures, the mushroom-like

patch size is 3 mm and the gap between the patches is 0.5 mm. Four columns of mushroom-like patches are inserted between the antennas to reduce the mutual coupling.

The measured results are shown in Fig. 16. It is observed that both antennas resonate at 5.86 GHz with return loss better than -10 dB. For the antennas without the EBG structure, the mutual coupling at 5.86 GHz is -16.8 dB. In comparison, the mutual coupling of the antennas with the EBG structure is only -24.6 dB. An approximately 8 dB reduction of mutual coupling is achieved at the resonant frequency of 5.86 GHz. This result agrees well with the simulated result shown in Fig. 13(b). From this experimental demonstration, it can be concluded that the EBG structure can be utilized to reduce the antenna mutual coupling between array elements.

V. Conclusion

In this paper, a mushroom-like EBG structure is implemented in the design of microstrip antenna arrays to reduce the strong mutual coupling caused by the thick and high permittivity substrate without sacrificing the compact size or bandwidth of the antenna elements. The EBG structure is analyzed using the FDTD method. The near field distribution of the EBG structure clearly demonstrates its band-gap feature of suppressing surface waves. Also compared is the mutual coupling of microstrip antennas on various thickness and permittivities substrates. The strongest mutual coupling happens in the E-plane coupled antennas on a thick and high permittivity substrate due to the pronounced surface waves. The EBG structure is then inserted between the antenna elements to reduce the mutual coupling. Compared to other approaches such as cavity back structure, the EBG structure demonstrates a better performance to improve the mutual coupling. Several microstrip antennas are fabricated to validate this observation, and an 8 dB mutual coupling reduction is observed at the resonant frequency. This mutual coupling reduction technique can be used in various antenna array applications.

References

[1] Y. Rahmat-Samii and H. Mosallaei, "Electromagnetic band-gap structures: Classification, characterization and applications," in *Proc. Inst. Elect. Eng.-ICAP Symp.*, Apr. 2001, pp. 560–564.

[2] E. Yablonovitch, "Photonic crystals," *J. Modern Opt.*, vol. 41, no. 2, pp. 173–194, 1994.

[3] D. Sievenpiper, L. Zhang, R. F. J. Broas, N. G. Alexopolus, and E. Yablonovitch, "High-impedance electromagnetic surfaces with a forbidden frequency band," *IEEE Trans. Microwave Theory Tech.*, vol. 47, pp. 2059–2074, Nov. 1999.

[4] D. Sievenpiper, J. Schaffner, B. Loo, G. Tangonan, R. Harold, J. Pikulski, and R. Garcia, "Electronic beam steering using a varactor-tuned impedance surface," in *Proc. IEEE AP-S Dig.*, vol. 1, July 2001, pp. 174–177.

[5] A. S. Barlevy and Y. Rahmat-Samii, "Characterization of electromagnetic band-gaps composed of multiple periodic tripods with interconnecting vias: Concept, analysis, and design," *IEEE Trans. Antennas Propagat.*, vol. 49, pp. 343–353, Mar. 2001.

[6] F. Yang and Y. Rahmat-Samii, "Step-Like structure and EBG Structure to improve the performance of patch antennas on high dielectric substrate," in *Proc. IEEE AP-S Dig.*, vol. 2, July 2001, pp. 482–485.

[7] R. Gonzalo, P. Maagt, and M. Sorolla, "Enhanced patch-antenna performance by suppressing surface waves using photonic-bandgap substrates," *IEEE Trans. Microwave Theory Tech.*, vol. 47, pp. 2131–2138, Nov. 1999.

[8] F. Yang and Y. Rahmat-Samii, "Mutual coupling reduction of microstrip antennas using electromagnetic band-gap structure," in *Proc. IEEE AP-S Dig.*, vol. 2, July 2001, pp. 478–481.

[9] M. Rahman and M. Stuchly, "Wide-band microstrip patch antenna with planar PBG structure," in *Proc. IEEE AP-S Dig.*, vol. 2, July 2001, pp. 486–489.

[10] R. Coccioli, F. R. Yang, K. P. Ma, and T. Itoh, "Aperture-coupled patch antenna on UC-PBG substrate," *IEEE Trans. Microwave Theory Tech.*, vol. 47, pp. 2123–2130, Nov. 1999.

[11] S. Sharma and L. Shafai, "Enhanced performance of an aperture-coupled rectangular microstrip antenna on a simplified unipolar compact photonic bandgap (UCPBG) structure," in *Proc. IEEE AP-S Dig.*, vol. 2, July 2001, pp. 498–501.

[12] Z. Li and Y. Rahmat-Samii, "PBG, PMC and PEC surface for antenna applications: A comparative study," in *Proc. IEEE AP-S Dig.*, July 2000, pp. 674–677.

[13] F. Yang and Y. Rahmat-Samii, "A low profile circularly polarized curl antenna over Electromagnetic Band-Gap (EBG) surface," *Microw. Opt. Tech. Lett.*, vol. 31, no. 4, pp. 478–481, Nov. 2001.

[14] J. Y. Park, C. C. Chang, Y. Qian, and T. Itoh, "An improved low-profile cavity-backed slot antenna loaded with 2D UC-PBG reflector," in *Proc. IEEE AP-S Dig.*, vol. 4, July 2001, pp. 194–197.

[15] M. A. Jensen and Y. Rahmat-Samii, "Performance analysis of antennas for hand-held transceivers using FDTD," *IEEE Trans. Antennas Propagat.*, vol. 42, pp. 1106–1113, Aug. 1994.

[16] G. P. Gauthier, A. Courtay, and G. H. Rebeiz, "Microstrip antennas on synthesized low dielectric-constant substrate," *IEEE Trans. Antennas Propagat.*, vol. 45, pp. 1310–1314, Aug. 1997.

[17] I. Papapolymerou, R. F. Frayton, and L. P. B. Katehi, "Micromachined patch antennas," *IEEE Trans. Antennas Propagat.*, vol. 46, pp. 275–283, Feb. 1998.

[18] J. S. Colburn and Y. Rahmat-Samii, "Patch antennas on externally perforated high dielectric constant substrates," *IEEE Trans. Antennas Propagat.*, vol. 47, pp. 1785–1794, Dec. 1999.

[19] D. R. Jackson, J. T. Williams, A. K. Bhattacharyya, R. L. Smith, S. J. Buchheit, and S. A. Long, "Microstrip patch antenna designs that do not excite surface waves," *IEEE Trans. Antennas Propagat.*, vol. 41, pp. 1026–1037, Aug. 1993.

[20] R. P. Jedlicka, M. T. Poe, and K. R. Carver, "Measured mutual coupling between microstrip antennas," *IEEE Trans. Antennas Propagat.*, vol. 29, pp. 147–149, Jan. 1981.

[21] D. F. Sievenpiper, "High-impedance electromagnetic surfaces," Ph.D. dissertation, UCLA, 1999.

[22] M. Rahman and M. A. Stuchly, "Transmission line-periodic circuit representation of planar microwave photonic bandgap structures," *Microwave Opt. Technol. Lett.*, vol. 30, no. 1, pp. 15–19, July 2001.

[23] F. Yang and Y. Rahmat-Samii, "Reflection phase characterization of an electromagnetic band-gap (EBG) surface," in *Proc. IEEE AP-S Dig.*, vol. 3, June 2002, pp. 744–747.

[24] Y. X. Guo, K. M. Luk, and K. W. Leung, "Mutual coupling between rectangular dielectric resonator antennas by FDTD," *Proc. Inst. Elect. Eng.- Microwave Antennas Propagation*, vol. 146, no. 4, pp. 292–294, Aug. 1999.

[25] D. E. Humphrey and V. F. Fusco, "A mutual coupling model for microstrip patch antenna pairs with arbitrary orientation," *Microw. Opt. Tech. Lett.*, vol. 18, pp. 230–233, June 1998.

[26] D. H. Schaubert and K. S. Yngvesson, "Experimental study of a microstrip array on high permittivity substrate," *IEEE Trans. Antennas Propagat.*, vol. 34, pp. 92–97, Jan. 1986.

[27] D. H. Schaubert, D. M. Pozar, and A. Adrian, "Effect of microstrip antenna substrate thickness and permittivity: Comparison of theories with experiment," *IEEE Trans. Antennas Propagat.*, vol. 37, pp. 677–682, June 1989.

Fan Yang (S'96–M'03) received the B.S. and M.S. degrees from Tsinghua University, Beijing, China and the Ph.D. degree from University of California, Los Angeles, all in electric engineering, in 1997, 1999, and 2002, respectively.

From 1994 to 1999, he was a Research Assistant with the State Key Laboratory of Microwave and Digital Communications, Tsinghua University, China. From 1999 to 2002, he was a Graduate Student Researcher in the Antenna Research, Applications, and Measurement Laboratory (ARAM), University of California, Los Angeles. Since September 2002, he has been a Research Engineer in the UCLA Antenna Laboratory. His research interests include microstrip antenna and reconfigurable antenna designs, electromagnetic band-gap structures, numerical methods in electromagnetics, and antenna measurement techniques.

Dr. Yang is Secretary of the IEEE AP Society, Los Angeles chapter.

Yahya Rahmat-Samii (S'73–M'75–SM'79–F'85) received the M.S. and Ph.D. degrees in electrical engineering from the University of Illinois, Urbana-Champaign.

He is a Professor and the Chairman of the Electrical Engineering Department, University of California, Los Angeles (UCLA). He was a Senior Research Scientist at NASA's Jet Propulsion Laboratory/California Institute of Technology, Pasadena, before joining UCLA in 1989. He was a Guest Professor with the Technical University of Denmark (TUD) during the summer of 1986. He has also been a consultant to many aerospace companies. He has been Editor and Guest Editor of many technical journals and book publication entities. He has Authored and Coauthored more than 500 technical journal articles and conference papers and has written 17 book chapters. He is the Coauthor of two books entitled, *Electromagnetic Optimization by Genetic Algorithms, and Impedance Boundary Conditions in Electromagnetic*s published in 1999 and 1995, respectively. He is also the holder of several patents. He has had pioneering research contributions in diverse areas of electromagnetics, antennas, measurement and diagnostics techniques, numerical and asymptotic methods, satellite and personal communications, human/antenna interactions, frequency selective surfaces, electromagnetic band-gap structures and the applications of the genetic algorithms, etc., (visit http://www.antlab.ee.ucla.edu). On several occasions, his work has made the cover of many magazines and has been featured on several TV newscasts.

Dr. Rahmat-Samii was the elected 1995 President and 1994 Vice-President of the IEEE Antennas and Propagation Society. He was appointed an IEEE Antennas and Propagation Society Distinguished Lecturer and presented lectures internationally. He was elected as a Fellow of the Institute of Advances in Engineering (IAE) in 1986. He was also a member of the Strategic Planning and Review Committee (SPARC) of the IEEE. He was the IEEE AP-S Los Angeles Chapter Chairman (1987–1989) and his chapter won the Best Chapter Awards in two consecutive years. He has been the plenary and millennium session speaker at many national and international symposia. He was one of the directors and Vice President of the Antennas Measurement Techniques Association (AMTA) for three years. He has also served as Chairman and Co-Chairman of several national and international symposia. He was also a member of UCLA's Graduate council for a period of three years. For his contributions, he has received numerous NASA and JPL Certificates of Recognition. In 1984, he received the coveted Henry Booker Award of the International Scientific Radio Union (URSI) which is given triennially to the Most Outstanding Young Radio Scientist in North America. Since 1987, he has been designated every three years as one of the Academy of Science's Research Council Representatives to the URSI General Assemblies held in various parts of the world. In 1992 and 1995, he was the recipient of the Best Application Paper Prize Award (Wheeler Award) for papers published in the 1991 and 1993 IEEE ANTENNAS AND PROPAGATION. In 1993, 1994, and 1995, three of his Ph.D. students were named the Most Outstanding Ph.D. Students at UCLA's School of Engineering and Applied Science. Seven others received various Student Paper Awards at the 1993–2002 IEEE AP-S/URSI Symposiums. He is a Member of Commissions A, B, J, and K of USNC/URSI, AMTA, Sigma Xi, Eta Kappa Nu, and the Electromagnetics Academy. He is listed in *Who's Who in America*, *Who's Who in Frontiers of Science and Technology*, and *Who's Who in Engineering*. In 1999, he was the recipient of the University of Illinois ECE Distinguished Alumni Award. In 2000, he was the recipient of IEEE Third Millennium Medal and AMTA Distinguished Achievement Award. In 2001, he was the recipient of the Honorary Doctorate in physics from the University of Santiago de Compostela, Spain. In 2001, he was elected as the Foreign Member of the Royal Academy of Belgium for Science and the Arts. He is the designer of the IEEE Antennas and Propagation Society logo that is displayed on all IEEE ANTENNAS AND PROPAGATION publications.